Reconfigurable Adaptive Array Beamforming by Antenna Selection

Xiangrong Wang*, Elias Aboutanios, Senior Member, Matthew Trinkle and Moeness G. Amin, Fellow

***Abstract*—Traditional adaptive array beamforming with a fixed array configuration can lead to significant inefficiencies and performance loss under different scenarios. As antennas become smaller and cheaper relative to front-ends, it becomes important to devise a reconfigurable adaptive antenna array (RAAA) strategy to yield high signal to noise and interference ratio using fewer antennas. This is achieved by selecting K from N antennas to minimize the Spatial Correlation Coefficient (SCC) between the desired signal and the interference. The lower bound of optimum SCC is formulated with two relaxation methods to give information about the suitable number of selected antennas K. A Correlation Measurement (CM) method is proposed to select the optimum subarray with K antennas, thereby reducing complexity. We carry out performance analysis and show that a $1/K^2$-suboptimum solution can be guaranteed with arbitrary shaped arrays. Furthermore, a Difference of Convex Sets (DCS) method is proposed to select the optimum subarray with controlled quiescent pattern in order to reduce the effect of interference during the reconfiguration time. The utility of the proposed array reconfiguration for performance improvement without increasing the cost is demonstrated using both simulated and experimental data.**

***Index Terms*—Antenna Selection, Adaptive Array Beamforming, Convex Optimization, Correlation Measurement, Difference of Convex Sets**

I. Introduction

A. Motivation

Adaptive array processing plays an important role in diverse application areas, such as radar, sonar systems and wireless communication. Adaptive arrays are capable of spatial filtering, which makes it possible to receive the desired signal from a particular direction while simultaneously blocking the interference from another direction [1]. However, the high cost of an entire front-end per antenna makes large array beamforming very expensive, for example for a phased array radar with hundreds of antennas. Antenna elements, on the other hand, are becoming smaller and cheaper. In Global Navigation Satellite Systems (GNSS), adaptive array processing has also proved to be very promising and a potentially effective approach for combating multipath and interference. It has been long known that increasing the number of front-ends enables the formation of narrower beams. As a result, the benefits afforded by using more front-ends are only gained at the cost of increasingly complex and expensive receiver hardware [2]. Therefore, antenna selection strategies are becoming increasingly desirable. Existing techniques consider the array configuration to be fixed and focuses on developing adaptive beamforming and filtering techniques [3], [4], [5]. As the array configuration is also a potential degree of freedom (DOF), it plays a fundamental role in the performance of array beamforming. In this paper, a reconfigurable adaptive antenna array (RAAA) strategy is proposed, which can reduce the cost incurred by many front-ends, while best preserving the desired performance. This strategy is studied in the context of GNSS applications.

The block diagram of the proposed RAAA strategy by antenna selection is shown in Fig. 1. There are only K ($K \ll N$) front-ends installed in the receiver. In general, the procedure is as follows. We initially compose a K-antenna subarray which gives the lowest estimation variance (such subarray usually has symmetry with respect to the x or y axis and includes the extreme antennas with largest aperture length [6], [7]). The receiver obtains rough Direction of Arrival (DOA) estimates for the desired signal and interference. The optimum array configuration is then derived from the estimated DOAs. The selected K antennas are switched on and connected to the K front-ends, while the de-selected antennas are kept off or connected to a matched load. In the case of GNSS, the receiver is able to decode the navigation data, and obtain the DOA of the satellites with high accuracy. The DOA of interference, on the other hand, needs to be estimated prior to the adaptive array processing step. Subsequently, a new iteration of adaptive beamforming is applied based on the optimum subarray. Thus, the hardware cost of front-ends is kept to a minimum, and the computational load associated with the inverse of covariance matrix is reduced. This is accomplished by identifying and selecting the optimum array configuration, which corresponds to the best performance of K-antenna subarrays.

B. Background

Synthesizing a desired beampattern by changing the array configuration is an important problem with diverse applications. A discrete antenna selection method was recently proposed to synthesize a desired beampattern with the fewest possible antennas. There exist effective methods to solve this problem, such as a heuristic method [8], a convex optimization method [9], [10], [11], a Bayesian Compressive Sensing method [12], a Matrix Pencil method [13] and an Iterative FFT algorithm [14], [15] etc. These weight synthesis techniques

X. Wang* and E. Aboutanios are with the School of Electrical Engineering and Telecommunication, University of New South Wales, Sydney, Australia 2052. e-mail:x.r.wang@unsw.edu.au; elias@unsw.edu.au.

M. Trinkle is with the School of Electrical and Electronic Engineering, University of Adelaide, SA 5005, Australia. e-mail: mtrinkle@eleceng.adelaide.edu.au.

M. G. Amin is with the Center for Advanced Communications, College of Engineering, Villanova University, Villanova, PA 19085, USA. e-mail: moeness.amin@villanova.edu.

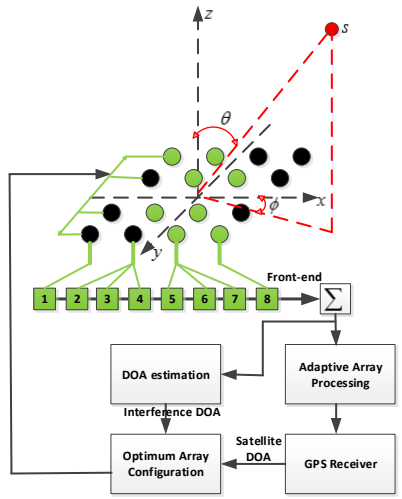

Fig. 1. Block diagram of RAAA strategy with the green circle selected and the dark one discarded: The DOAs of the satellite and interference are estimated and used to obtain the optimum sub-array. The selected antennas are then connected to the available front-ends. In this illustration, 8 front-ends are available and an 8-antenna subarray is selected out of a 16-antenna array.

are referred to as deterministic design approaches [16]. In contrast there is little research work relating data dependent adaptive array processing with array reconfiguration. Hence, we proceed in this work to combine an antenna selection strategy that "chooses K from N antennas" using switches, with adaptive array beamforming in order to enhance the performance of traditional array processing.

Since the number K of selected antennas is an important factor in the array processing performance, it should be considered carefully. The first part of this paper focuses on a theoretical analysis of the proposed RAAA strategy. In particular, we solve the problem of determining the suitable value of K with the aim of obtaining the best compromise between performance and cost. To this end, the spatial correlation coefficient (SCC), which characterises the spatial separation between the desired signal and interference is introduced and the lower bound of the optimal SCC is formulated using two convex relaxation methods. These two methods, namely Lagrange Dual and Semi-Definite Programming (SDP) relaxation, were primarily motivated in multicast applications [17], [18]. Since the detection performance of GNSS receivers is closely related to the effective carrier to noise density ratio (effective C/N_0), we derive in closed form the relationship between the effective C/N_0 and the SCC. The trade-off curve of the effective C/N_0 and the computational cost with respect to K gives the most suitable value of K with the best compromise.

The second part of this paper develops a method to choose the optimum K-antenna subarray from $C_N^K = \frac{N!}{K!(N-K)!}$ possible combinations. Searching every possible configuration by enumeration is very computationally expensive even for moderate N. Thus an effective method of solving the resulting NP-hard problem is necessary. The deterministic methods in [9]-[16] cannot be utilised in the underlying problem due to the existence of the binary constraint which requires each entry of the selection vector to be either zero or one. Additionally, the extra cardinality constraint, i.e. the requirement to activate exactly K antennas, makes this problem much more complicated. The popular Gaussian randomization method after the SDP relaxation for solving homogeneous quadratic optimization can be used to obtain the binary entry by projecting the solution into the feasible set [19], but the number of entries equal to one is not controllable. The upper bound calculation of the branch and bound method [20], the feasibility cutting with respect to binary constraints of cutting plane method [21] and the recursive structure of dynamic programming [22] are not suitable for real-time applications. Therefore, a simple greedy approach, called Correlation Measurement (CM) method, is adopted in this paper to solve the antenna selection problem for single interference case. Both mathematical analysis and simulation results show that the CM algorithm can return a feasible solution that is at least $1/K^2$-suboptimum for arbitrary shaped arrays. Subsequently, another method of solving the 0/1 integer programming, called Difference of Convex Sets (DCS), is proposed to select the optimum subarray with a null towards the interference and a controlled quiescent pattern. Although the DCS method is more computationally expensive, the effect of interferers during reconfiguration time is reduced for DCS optimum subarrays.

C. Contributions

Although this paper only takes GNSS application as an example to illustrate our proposed RAAA strategy, it is a general topic and can be applied in many other applications with antenna arrays. We focus only on the single interference case which is fundamental to the solution of the multiple-interference problem (this is beyond the scope of this paper and will be the subject of future work.) This paper makes a number of contributions: (i) We derive the non-linear relationship between the effective C/N_0 and the number of selected antennas K and utilize it to prove that the optimum subarray can maximally preserve the performance with reduced cost; (ii) We formulate the lower bound of the optimum SCC to obtain the suitable number of selected antennas for achieving the required compromise between the performance and cost; (iii) We present a modified CM method to select the optimum subarray with minimum SCC value and analyse its performance; (iv) We propose a DCS method to solve the 0/1 integer programming problem and reconfigure an optimum subarray with controlled quiescent pattern; (v) We demonstrate the utility of array reconfiguration for performance improvement by a comprehensive simulation of all the algorithms and data set from real experiments.

The remainder of this paper is organised as follows. In Section II the SCC is introduced, and the relationship between it and the effective C/N_0 is described. In Section III, the lower bound of the optimal SCC is formulated with two relaxation methods to indicate the suitable number K of selected antennas. The proposed CM method, its performance analysis and the DCS method are described in Section IV. In Section V and Section VI, a set of representative numerical results and real experimental results are reported and discussed respectively. Finally, some conclusions are drawn in Section VII.

II. Spatial Correlation Coefficient

The impact of the interference on the desired signal in GNSS applications can be characterized by the effective C/N_0, [23]. In addition to the Doppler separation, the spatial dimension also plays a vital part in the effective C/N_0 in the antenna array case [24], [25]. The array configuration, in particular, is fundamental to the overall performance of the receiver. Its effect on the performance is embodied in the spatial separation coefficient (SCC) [26], [27], which expresses the spatial separation between the desired signal and the interference with respect to the array. Below, we formulate the relationship between the SCC and the effective C/N_0.

Consider an N-antenna uniformly spaced array placed on the x-y plane with inter-element spacing d (A 4×4 planar array is shown in Fig.1). Let the elevation and azimuth angles of the desired signal and interference be given by (θ_s, ϕ_s) and (θ_j, ϕ_j) respectively. Then, the **u**-space DOA parameters are defined as

$$\mathbf{u}_i = [\sin\theta_i \cos\phi_i \quad \sin\theta_i \sin\phi_i]^T, \quad \text{for } i = s, j \tag{1}$$

where ^{T} is the transpose. The steering vectors of the desired signal and interference are

$$\mathbf{v}_s = e^{j\frac{2\pi}{\lambda}\mathbf{P}\mathbf{u}_s}, \quad \mathbf{v}_j = e^{j\frac{2\pi}{\lambda}\mathbf{P}\mathbf{u}_j}, \tag{2}$$

where the matrix $\mathbf{P} = [\mathbf{p}_1, \mathbf{p}_2, ..., \mathbf{p}_N]^T \in R^{N\times 2}$ contains the coordinates of antenna elements,

$$\mathbf{P} = \begin{bmatrix} x_1 & y_1 \\ x_2 & y_2 \\ \vdots & \vdots \\ x_N & y_N \end{bmatrix}. \tag{3}$$

Under the assumption that the noise and interference are uncorrelated, their covariance matrix is given by

$$\mathbf{R}_n = \sigma^2\mathbf{I} + P_j\mathbf{v}_j\mathbf{v}_j^H, \tag{4}$$

where σ^2 is the thermal noise power, P_j is the interference power and the superscript ^{H} denotes the conjugate transpose operation. Applying the Sherman-Morrison-Woodbury formula to the inverse covariance matrix Eq. (4) yields

$$\begin{aligned} \mathbf{R}_n^{-1} &= \sigma^{-2}(\mathbf{I} - \frac{\mathbf{v}_j\mathbf{v}_j^H}{\frac{\sigma^2}{P_j} + \mathbf{v}_j^H\mathbf{v}_j}), \\ &= \sigma^{-2}(\mathbf{I} - \frac{\mathbf{v}_j\mathbf{v}_j^H}{\frac{\sigma^2}{P_j} + N}). \end{aligned} \tag{5}$$

Here, we have assumed, without loss of generality, that $\mathbf{v}_j^H\mathbf{v}_j = \mathbf{v}_s^H\mathbf{v}_s = N$. Define the parameter SCC as

$$\alpha_{js} = \frac{\mathbf{v}_j^H\mathbf{v}_s}{\|\mathbf{v}_j\|\|\mathbf{v}_s\|} = \frac{\mathbf{v}_j^H\mathbf{v}_s}{\sqrt{\mathbf{v}_j^H\mathbf{v}_j}\sqrt{\mathbf{v}_s^H\mathbf{v}_s}} = \frac{\mathbf{v}_j^H\mathbf{v}_s}{N}. \tag{6}$$

It is clear that $|\alpha_{js}| \leq 1$ and the SCC can be interpreted as the cosine of the angle ϑ between the desired signal and the interference as shown in Fig. 2. Small values of absolute SCC indicate spatial dissimilarity between the desired signal and interference, and orthogonality is achieved when SCC is zero. Using Eqs. (5) and (6), the optimum weight vector is given by

$$\begin{aligned} \mathbf{w}_{opt} &= \gamma\mathbf{R}_n^{-1}\mathbf{v}_s, \\ &= \frac{\gamma}{\sigma^2}(\mathbf{v}_s - \frac{\mathbf{v}_j\alpha_{js}}{\frac{\sigma^2}{NP_j} + 1}), \end{aligned} \tag{7}$$

where γ is a constant that does not affect the output performance. Finally, the corresponding output SINR becomes [28],

$$\begin{aligned} \text{SINR}_{out} &= P_s\mathbf{v}_s^H\mathbf{R}_n^{-1}\mathbf{v}_s, \\ &= \frac{NP_s}{\sigma^2}(1 - |\alpha_{js}|^2\frac{\frac{NP_j}{\sigma^2}}{1 + \frac{NP_j}{\sigma^2}}), \\ &= N\text{SNR}(1 - |\alpha_{js}|^2\varrho), \end{aligned} \tag{8}$$

where P_s denotes the signal power and $\text{SNR} = P_s/\sigma^2$. ϱ is an interference to noise figure given in terms of the interference to noise ratio ($\text{INR} = P_j/\sigma^2$) as

$$\varrho = \frac{N\text{INR}}{1 + N\text{INR}}. \tag{9}$$

The interference to noise figure ϱ characterises the relative effects of the white noise and interference on the array performance. It satisfies $0 \leq \varrho < 1$. A value that is close to 0 indicates that the white noise is the dominant source of performance degradation, and a value close to 1 implies that the interference dominates the noise. We now make the following observations:

1) When the noise is dominant, ϱ is close to 0 and the effect of the SCC is suppressed. In this case, the SINR_{out} is linear with the number of array elements N. Therefore, choosing a smaller subarray can incur a significant performance loss.
2) If ϱ is large (close to 1), the interference is dominant and the effect of the SCC is pronounced. Then the optimum weight vector $\mathbf{w}_{opt}$ lies in the interference nullspace. As a result, the spatial filter will also suppress the interference directional component of the desired signal. Therefore, choosing a smaller subarray that minimises the SCC, i.e. makes the interference and the desired signal identically or approximately orthogonal with respect to the array configuration, may only incur a small performance loss as compared with the full array.

Since our focus here is interference mitigation, we assume the interference is much stronger than the noise in the rest part of the paper. The SINR_{out} at the output of adaptive array filter shown in Eq. (8) is the measurement before cross correlation with the locally generated pseudo-random code. Because GNSS receivers adopt a direct sequence spread spectrum (DSSS) processing technique, the effective C/N_0, given as the total GPS signal power divided by the noise power in a 1Hz bandwidth, is recommended as a performance measure. Converting Eq. (8) into effective C/N_0 value gives (here $\varrho \doteq 1$):

$$(C/N_0)_{\text{eff}} = \frac{NP_s^d}{G_nN_0}(1 - |\alpha_{js}|^2), \tag{10}$$

where P_s^d is the satellite signal power after pseudo-random code de-spreading, N_0 is the white noise power density per

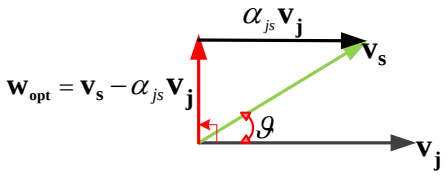

Fig. 2. Relationship between SCC and adaptive array weight vector.

Hz and G_n is the noise processing gain. Eq. (10) shows that when the number of antennas N is fixed, the effective C/N_0 can be improved by changing the array configuration to reduce the SCC value. Thus the SCC characterizes the effect of the array configuration on the array processing performance. Also note that the relationship between effective C/N_0 and the number of available antennas is not linear because the SCC also depends on the number of antennas by Eq. (6).

III. Lower Bound of Optimum SCC for Single Interference

The mathematical model of antenna selection problem is choosing K from N antennas to compose a subarray that minimizes the SCC value. Let $\mathbf{x}$ be a selection vector with N elements whose value can only be 0 (not selected) or 1 (selected). Thus the SCC expression based on the selected subarray with K antenna elements can be expressed as

$$|\alpha_{js}| = \frac{|\mathbf{x}^T\mathbf{v}_{js}|}{K} \Leftrightarrow |\alpha_{js}|^2 = \frac{\mathbf{x}^T\mathbf{W}_r\mathbf{x}}{K^2}. \tag{11}$$

where $\mathbf{v}_{js}$ is the correlation steering vector defined as

$$\mathbf{v}_{js} = e^{j\frac{2\pi}{\lambda}\mathbf{P}(\mathbf{u}_s - \mathbf{u}_j)}, \tag{12}$$

and $\mathbf{W}_r = \text{real}(\mathbf{v}_{js}\mathbf{v}_{js}^H)$. The antenna selection problem can then be cast as a two-way partitioning model [29] as follows:

$$\min |\alpha_{js}|^2, \tag{13a}$$

$$\text{s.t. } x_i(x_i - 1) = 0 \quad i = 1...N, \tag{13b}$$

$$\text{and } \mathbf{x}^T\mathbf{x} = K. \tag{13c}$$

Due to the existence of binary constraints in Eq. (13b), the primal problem above is not a convex optimization (it is a 0/1 integer optimization). Thus, we resort to relaxation methods to get the lower bound of the optimal value. There are two kinds of commonly used relaxation methods: Lagrange Dual Relaxation and Direct Semidefinite Programming (SDP) relaxation. The Lagrange Dual Relaxation utilizes weak duality and the convexity of duals to obtain the lower bound, whereas the Direct SDP Relaxation deletes the rank-one matrix constraint to obtain a bound. We formulate these two methods and discuss the relationship between them.

A. Lagrange Dual Relaxation Method

Now proceeding with the analysis, the Lagrangian is

$$L(\mathbf{x}, \boldsymbol{\mu}, \upsilon) = \mathbf{x}^T(\frac{1}{K^2}\mathbf{W}_r + diag(\boldsymbol{\mu}) + \upsilon\mathbf{I})\mathbf{x} - \boldsymbol{\mu}^T\mathbf{x} - K\upsilon. \tag{14}$$

The Lagrange Dual function for the minimization of $L(\mathbf{x}, \boldsymbol{\mu}, \upsilon)$ over $\mathbf{x}$ becomes

$$g(\boldsymbol{\mu}, \upsilon) = \inf_{\mathbf{x}}\{L(\mathbf{x}, \boldsymbol{\mu}, \upsilon)\} \tag{15}$$
$$= \begin{cases} -\frac{1}{4}\boldsymbol{\mu}^T(\frac{1}{K^2}\mathbf{W}_r + diag(\boldsymbol{\mu}) + \upsilon\mathbf{I})^{-1}\boldsymbol{\mu} - K\upsilon, \\ \text{if } \frac{1}{K^2}\mathbf{W}_r + diag(\boldsymbol{\mu}) + \upsilon\mathbf{I} \succeq 0 \\ \text{and } \boldsymbol{\mu} \in \mathcal{R}(\frac{1}{K^2}\mathbf{W}_r + diag(\boldsymbol{\mu}) + \upsilon\mathbf{I}); \\ -\infty \qquad\qquad otherwise. \end{cases}$$

where $\mathcal{R}(\bullet)$ means the column space of the matrix $\bullet$. It is evident that the Lagrange dual function in Eq. (15) is a concave function. Using the Schur complement, we can express Eq. (15) as a linear matrix inequality (LMI),

$$\begin{aligned} \max \quad & \zeta, \\ \text{s.t.} \quad & \begin{bmatrix} \frac{1}{K^2}\mathbf{W}_r + diag(\boldsymbol{\mu}) + \upsilon\mathbf{I} & -\frac{1}{2}\boldsymbol{\mu} \\ -\frac{1}{2}\boldsymbol{\mu}^T & -K\upsilon - \zeta \end{bmatrix} \succeq 0. \end{aligned} \tag{16}$$

The dual problem (16) is a Semidefinite Programming (SDP) with three variables ζ, υ and $\boldsymbol{\mu}$ and can be effectively solved using the interior point based optimization method through CVX [30]. Therefore, after calculating the maximum value of $g_{max}(\tilde{\boldsymbol{\mu}}, \tilde{\upsilon})$, the lower bound of the optimal SCC is

$$|\alpha_{js}|^2_{min} \geq g_{max}(\tilde{\boldsymbol{\mu}}, \tilde{\upsilon}), \tag{17}$$

where $\tilde{\upsilon}$ and $\tilde{\boldsymbol{\mu}}$ are dual optimal solutions. Now in order to derive the final relationship between the effective C/N_0 and K, we proceed to substitute Eq. (17) into Eq. (10). Thus, the upper bound of the effective C/N_0 becomes

$$(C/N_0)_{\text{eff}} \leq \frac{KP_s^d}{G_nN_0}(1 - g_{max}(\tilde{\boldsymbol{\mu}}, \tilde{\upsilon})). \tag{18}$$

Eq. (18) asserts that none of the K-antenna arrays can achieve better performance than the upper bound calculated from the lower bound of the optimum SCC. Furthermore, this equation shows the trade-off between the bound on achievable performance and the computational cost which increases with the number of antennas. Therefore, Eq. (18) gives a way to determine the suitable number of selected antennas K under different scenarios as a direct result of this trade-off between cost and performance. This point will be elaborated further in the simulation results.

B. Direct SDP Relaxation Method

In addition to the Lagrange Dual Relaxation method, there is another commonly used direct SDP Relaxation method that relaxes the original problem by deleting the rank-one constraint. Thus, the optimisation problem is cast as,

$$\min \frac{1}{K^2}\text{tr}(\mathbf{X}\mathbf{W}_r), \tag{19a}$$

$$\text{s.t.} \begin{bmatrix} \mathbf{X} & \mathbf{x} \\ \mathbf{x}^T & 1 \end{bmatrix} \succeq 0, \tag{19b}$$

$$\text{tr}(\mathbf{X}\mathbf{E}_i) - \mathbf{e}_i^T\mathbf{x} = 0, \ i = 1, 2...N, \tag{19c}$$

$$\text{tr}(\mathbf{X}) = K. \tag{19d}$$

where the optimization variables are $\mathbf{X} \in R^{N\times N}$ and $\mathbf{x} \in R^N$, vector $\mathbf{e}_i \in R^N$ is the i_{th} unit vector with the i_{th} entry being

TABLE I
CORRELATION MEASUREMENT ALGORITHM

Step 1	Set all candidate antennas selected, i.e. $\mathbf{x} = \mathbf{1}^N$ and iteration number $k = 0$,
Step 2	Let $i := \arg\max_{l=1,\ldots,N} \sum_{j=1}^{N} \tilde{\mathbf{W}}_{jl}$,
Step 3	Delete sensor i, i.e. set $\mathbf{x}(i) = 0$, Set the i_{th} column and i_{th} row of $\tilde{\mathbf{W}}$ to zero, Put $k := k + 1$,
Step 4	If $k = N - K$, terminate, otherwise go back to Step 2.

one and all others being zero. The matrix $\mathbf{E}_i = \mathbf{e}_i\mathbf{e}_i^T$. The function tr($\bullet$) is the trace of the matrix $\bullet$.

Now we turn our attention to the relationship between the Lagrange Dual Relaxation Eq. (16) and the Direct SDP Relaxation Eq. (19). They are duals of each other according to [31], and therefore the two bounds are identical provided that Slater's condition is satisfied. In our specific problem, there is no duality gap between the pair of dual problems Eq. (16) and Eq. (19). The detailed derivation of strong duality is shown in Appendix A. The differences between the two relaxation methods are:

1) Eq. (13)$\rightarrow$ Eq. (16): dualizes $N+1$ constraints, producing a dual problem in R^{N+1};
2) Eq. (13)$\rightarrow$ Eq. (19): linearises $N+1$ constraints, producing Eq. (19) with N^2 extra variables.

Often the Lagrangian Duality Relaxation method is preferred due to its simplicity.

IV. Optimum Subarray Selection

The two relaxation methods cannot return a binary selection vector $\mathbf{x}$ due to the weak duality. Therefore, for single interference cases, we adopt a simple greedy search approach, called Correlation Measurement (CM) [32] to solve the selection problem due to its low complexity. However, since the CM method only places constraints on DOAs of the interference and desired signal, the resulting subarray response can exhibit high sidelobes even with grating lobes. Thus, we propose a Difference of Convex Sets (DCS) method to compose the optimum subarray with controlled quiescent pattern.

A. The CM method

The CM method adopts a bottom-up search strategy to reduce the candidate set size by deleting the candidate that is not in the optimum solution to the previous sub-problem. The squared SCC in Eq. (11) is equivalent to the sum of the selected entries of the matrix $\tilde{\mathbf{W}}_r$. That is

$$|\alpha_{js}|^2 = \mathbf{x}^T\tilde{\mathbf{W}}\mathbf{x} = \sum_{i,j=1}^{N} \mathbf{x}(i)\mathbf{x}(j)\tilde{\mathbf{W}}_{ij}, \tag{20}$$

where the matrix $\tilde{\mathbf{W}} = \frac{1}{K^2}\mathbf{W}_r$. Essentially, the CM method removes the antenna with the largest sum of correlation measurement relative to all remaining sensors in every iteration as shown in Table I.

It is difficult to derive a closed formula to describe the performance of the CM method because of negative entries of $\tilde{\mathbf{W}}$ (or the complex entries of $\mathbf{v}_{js}$) [22]. However, we can still arrive at some bounds on the performance as given by the following two theorems.

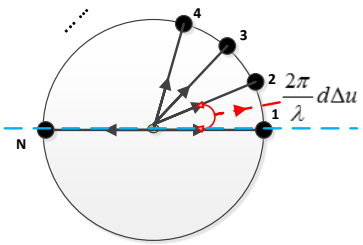

Fig. 3. Proof of Theorem 4.1: N antennas are denoted as N nodes on the unit circle. When the angle between every two successive nodes (distributed evenly around the circle) is less than $\frac{2\pi}{\lambda} d\Delta u$, all nodes are located in the upper half circle.

1) Theorem 4.1: For a uniformly spaced N-antenna linear array with inter-element spacing d, if the u-space DOA between the desired signal and the interference satisfies

$$|\Delta u| = |u_s - u_j| \leq \frac{1}{N-1}\frac{\lambda}{2d}, \tag{21}$$

then,

1) the CM method can always return a global optimum solution, and
2) the SCC value of a larger array is always greater than that of a smaller array.

Proof: The SCC in Eq. (11) can be expressed as the normalised sum of the selected exponentials in the polar coordinate system as shown in Fig. 3,

$$\alpha_{js} = \frac{1}{K}\sum_{i=1}^{N} \mathbf{x}(i)e^{j\frac{2\pi}{\lambda}(i-1)d\Delta u}. \tag{22}$$

Thus, it is evident that the SCC minimization problem is essentially to select K exponentials with opposite directions to cancel each other. When $\Delta u \leq \frac{1}{N-1}\frac{\lambda}{2d}$, all exponentials lie within the upper half of the circle. Thus the optimum subarray consists of the antennas at two extremes of the linear array, as a larger angle difference between two exponentials implies a smaller sum. Clearly, the sum of more exponentials is larger than the sum of fewer exponentials. Theorem 4.1 is a only sufficient but not necessary condition for global convergence. In fact, extensive simulations show that even when $|\Delta u|$ is much larger than $\frac{1}{N-1}\frac{\lambda}{2d}$, the CM method can still return a global optimum solution.

The next theorem will focus on deriving the upper bound of the distance between the CM local minimum and the global minimum when CM method does not converge globally.

2) Theorem 4.2: The distance between the objective value obtained by the CM method and the global minimum is upper bounded by $1/K^2$ for choosing K from N candidates when $|\Delta u|$ is sufficiently large.

The proof of Theorem 4.2 is shown in Appendix B. Now, since the CM method requires $\frac{1}{2}(N(N-1) - K(K-1))$ additions and $(N-1)(N-K)$ subtractions in total, its computational complexity is of order $O(N^2)$ operations for $K < N$. Therefore, the CM method has a low complexity,

making it both effective and efficient for solving the antenna selection problem in a single interference case.

B. Controlled Quiescent Pattern by DCS method

Although the CM method is highly suitable for selecting the optimum subarray, it only puts constraints on the null and mainlobe at the DOAs of the interference and the desired signal respectively. As a result, high sidelobes may occur in the synthesized beampattern due to the non-uniformly placed antennas. This is of concern and is addressed here via a new algorithm for solving the binary programming problem, called Difference of Convex Sets (DCS).

1) Theorem 4.3: The binary constraint $\mathbf{x} \in \{0,1\}^N$ is equivalent to the difference of two convex sets [33], i.e. $\mathbf{x} = A - B$ or the intersection between a convex and an inverse convex sets, i.e. $\mathbf{x} = A \cap B^c$, with

$$A: \quad \mathbf{x} \in [0,1]^N, \tag{23}$$

$$B: \quad \sum_{n=1}^{N} x_n^2 - \sum_{n=1}^{N} x_n = \mathbf{x}^T\mathbf{x} - \mathbf{1}^T\mathbf{x} < 0, \tag{24}$$

$$B^c: \quad \sum_{n=1}^{N} x_n - \sum_{n=1}^{N} x_n^2 = \mathbf{1}^T\mathbf{x} - \mathbf{x}^T\mathbf{x} \leq 0. \tag{25}$$

where $\mathbf{1} \in R^N$ is a vector with all entries being one.

Proof: The binary constraint $\mathbf{x} \in \{0,1\}^N$ is equivalent to

$$x_n^2 - x_n = 0, \ n = 1, 2, ..., N. \tag{26}$$

Eq. (26) results in $\mathbf{x}^T\mathbf{x} - \mathbf{1}^T\mathbf{x} = 0$. Eq. (23) implies $\mathbf{x}^T\mathbf{x} - \mathbf{1}^T\mathbf{x} \leq 0$, thus it is clear that $\mathbf{x} = A - B$. Furthermore constraint Eq. (23) together with constraint Eq. (25) result in constraint Eq. (26). □

According to Theorem 4.3, we can express binary constraints in Eq. (26) as a minimization problem ,i.e.

$$\min\{\mathbf{1}^T\mathbf{x} - \mathbf{x}^T\mathbf{x}\} = 0, \ \text{s.t.} \ 0 \leq \mathbf{x} \leq 1; \tag{27}$$

Or equivalently

$$\begin{aligned} \min \quad & \mathbf{1}^T\mathbf{x}, \\ \text{s.t.} \quad & \mathbf{x} \in [0,1]^N, \\ & \mathbf{x}^T\mathbf{x} = K. \end{aligned} \tag{28}$$

It is clear that the constraint $\mathbf{x}^T\mathbf{x} = K$ is not convex. Therefore we linearise it by the first-order Taylor decomposition. Since the derivative of $\mathbf{x}^T\mathbf{x}$ is $2\mathbf{x}$, the constraint $\mathbf{x}^T\mathbf{x} = K$ can be approximated in the $(k+1)_{th}$ iteration by the alternative form

$$2\mathbf{x}_k^T\mathbf{x} - \mathbf{x}_k^T\mathbf{x}_k = K, \tag{29}$$

Moreover, we sample the u-space DOA interval $[-1,1]$ to get the set of correlation vectors $\mathbf{v}_{js}^i, i = 1, ..., L$ defined in Eq. (12). Let us define desired SCC values for these samples as $\delta^i, i = 1, ..., L$. Then the subarray selection with controlled quiescent pattern in the $(k+1)_{th}$ iteration can be expressed as

$$\begin{aligned} \min \quad & \mathbf{1}^T\mathbf{x}, \\ \text{s.t.} \quad & |\mathbf{x}^T\mathbf{v}_{js}| \leq K\delta, \\ & |\mathbf{x}^T\mathbf{v}_{js}^i| \leq K\delta^i, i = 1, ..., L \\ & \mathbf{x} \in [0,1]^N, \\ & 2\mathbf{x}_k^T\mathbf{x} - \mathbf{x}_k^T\mathbf{x}_k = K. \end{aligned} \tag{30}$$

where $\mathbf{v}_{js}$ and $\delta \in [0,1]$ are the correlation vector and the desired SCC value corresponding to the arrival direction of the interference respectively. Then the iterative algorithm Eq. (30) can be solved by Linear Programming (LP) using the CVX toolbox. Since the minimum objective value is K and the corresponding optimum solution $\hat{\mathbf{x}}$ has binary entries, the termination condition is $\| \mathbf{x}_{k+1} - \mathbf{x}_k \|$ being small enough. It is shown in [34] that the sequence produced by Eq. (30) has non-increasing objective values. Therefore the iterative algorithm Eq. (30) will converge to the optimum solution $\hat{\mathbf{x}}$ which satisfies all the SCC value constraints, i.e. well controlled quiescent pattern. Finally, we point out that as the LP needs $O(n^2m)$ operations, where n and m are the numbers of variables and constraints respectively, the computational complexity of the DCS method is $O(N^3 + N^2L)$.

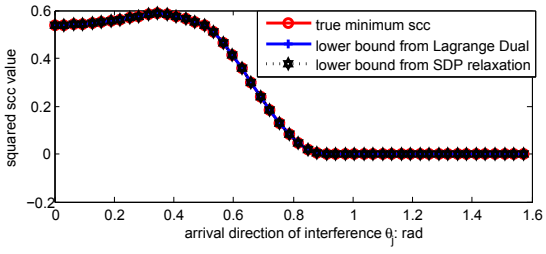

Fig. 4. Comparison between the true minimum SCC and lower bounds in different scenarios.

V. Simulation Results

In this section we present simulation results to validate the theory presented above.

A. Lower Bound Of Optimum SCC Under Different Scenarios

In the first example, we consider a 4×4 planar array with half wavelength inter-element spacing, as shown in Fig. 1, and proceed to choose the optimum subarray with $K = 8$ antennas with minimum SCC value. The desired signal is assumed to be coming from azimuth and elevation $\phi_s = 0.2\pi$ and $\theta_s = 0.1\pi$ respectively. The azimuth angle of the interference is set to be $\phi_j = 0.25\pi$ and the elevation angle, θ_j is varied from $\theta_j = 0$ to 0.5π. The comparison between the true minimum SCC and lower bounds obtained from the two methods under different scenarios is shown in Fig. 4, and clearly demonstrates that the calculated lower bounds of optimum SCC value are very tight in any scenario. Also observe that the two lower bounds are identical.

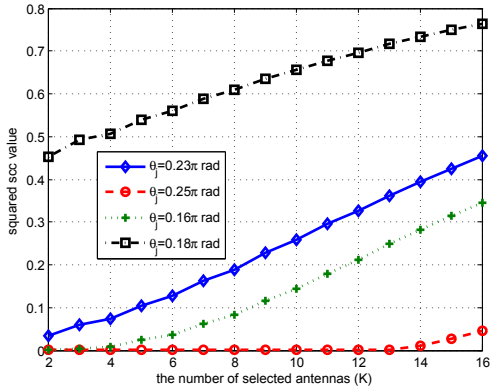

Fig. 5. Lower bound with different number of selected antennas in a 16-antenna half-wavelength spaced linear array.

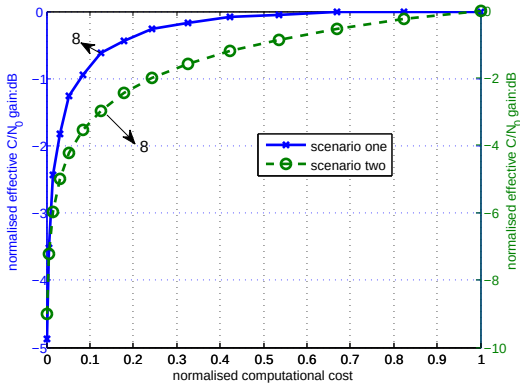

Fig. 6. Trade-off curve between the performance and the cost

B. Lower Bound Of Optimum SCC with Different Number of Selected Antennas

In the second example we investigate the dependence of the lower bound of optimum SCC on the number K of selected antennas using a 16-antenna half-wavelength spaced linear array. Supposing the desired signal is coming from $\theta_s = 0.2\pi\ rad$, the optimum SCC value with respect to different values of K were simulated under the following four different scenarios:

1) θ_j is 0.23π; $|\Delta u| < 1/15$;
2) θ_j is 0.25π; $|\Delta u| > 1/15$;
3) θ_j is 0.16π; $|\Delta u| > 1/15$;
4) θ_j is 0.18π; $|\Delta u| < 1/15$.

The simulation results are shown in Fig. 5. In this example, when $|\Delta u| \leq \frac{1}{N-1} = 1/15\ rad$, both the blue and the black curves are increasing with K. However when $|\Delta u| > \frac{1}{N-1}$, the optimum SCC value is nearly zero no matter how many antennas are selected as shown by the red curve. Interestingly, we find that the green curve is also increasing although $|\Delta u| > \frac{1}{N-1}$, the reason is Theorem 4.1 is only a sufficient but not necessary condition for global convergence.

C. The Optimum Number of Selected Antennas

In this example, we again use the 4×4 rectangular array to illustrate the method for finding a suitable value of K using the

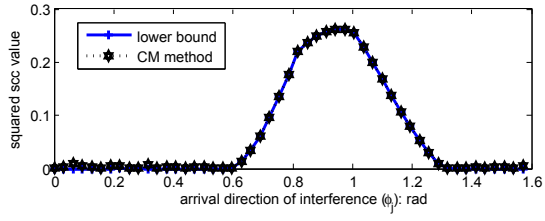

Fig. 7. Comparison between minimum SCC value of CM method and lower bound in a rectangular array.

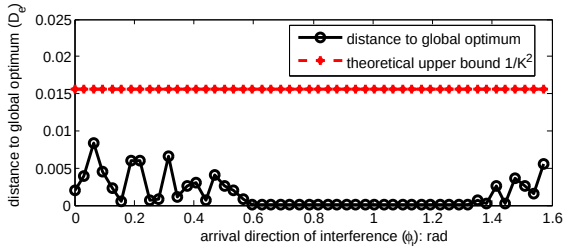

Fig. 8. Comparison between the error distance of CM method and upper bound in a rectangular array.

performance-cost trade-off curve. The most computationally expensive step for adaptive array processing is the inversion of the matrix which requires order K^3 complex operations, where K is the dimension of the covariance matrix. Thus, to appreciate the trade-off between the performance and computational cost, we calculate the normalised effective C/N_0 gain and computational cost by taking the entire full array as a reference. The suitable values of K for different compromises between the cost and performance can be found from this trade-off curve. In this simulation, the arrival direction of the desired signal is taken to be $\theta_s = 0.2\pi, \phi_s = 0.2\pi$ and the two DOAs of the interference are $\theta_j = 0.22\pi, \phi_j = 0.22\pi$ and $\theta_j = 0.4\pi, \phi_j = 0.4\pi$ for the first and second scenarios respectively. The simulation results are shown in Fig. 6. Observe that using an 8-antenna subarray saves 87.5% of computational cost with only 0.622dB performance degradation in scenario 1 and 2.971dB effective C/N_0 loss in scenario 2. This is a significant saving in computational load for a modest performance loss. Note that this does not take into account the additional hardware saving due to the reduction in the number of front ends, which is equal to the reduction in the number of antennas.

D. Validation of the CM method

Next we use the 4×4 uniform rectangular array to validate the effectiveness of proposed CM method. The arrival direction of the satellite signal is fixed at $\theta_s = 0.2\pi\ rad$ and $\phi_s = 0.3\pi\ rad$ and the elevation angle of the interference is fixed at $\theta_j = 0.3\pi\ rad$. The azimuth angle of the interference is changing from 0 to $0.5\pi\ rad$. The comparison result is shown in Fig. 7. According the Theorem 4.2, the upper bound of the distance between CM objective value to the global minimum is $\frac{1}{K^2} = 0.0156$ ($K = 8$ here). The result is shown in Fig. 8. It is clear that when the desired signal is close to the interference, the CM method can return a global optimum

solution. Moreover, when the two are well separated in space, the CM method can guarantee a $1/K^2$-suboptimum solution.

E. Performance Comparison

We now use a 50-antenna uniform linear array to show the performance of the proposed methods. We assume the desired signal and interference to arrive from 30° and 20° respectively, and set the signal to noise ratio to -20dB and interference to noise ratio to 10dB. In this example, we use a desired SCC value of 0.01 in the direction of the interference and 0.1 for all other angles of arrival. The optimum 32-antenna subarray returned by the CM method is shown in the upper plot of Fig. 9. The corresponding MVDR beampattern obtained by 1000 Monte Carlo trials is shown by the green dash-dot curve in Fig. 10. We can see that the peak sidelobe level (PSL) is -9.127dB with 4° mainlobe width and -80.87dB null-depth. The selected 32-antenna DCS subarray is shown in the middle plot of Fig. 9 and the MVDR beampattern with controlled quiescent pattern is represented in Fig. 10 by the solid blue curve. The null depth of -80.62dB is nearly the same as that of the CM method, but the peak sidelobe level (PSL) is now reduced to -16.5dB. This reduction in the PSL, however, comes at the cost of a slightly broader mainlobe with a width of 5.2°.

Most deterministic beampattern synthesis methods, such as [9] and [13]-[16], assume random antenna positions, which results in a greatly relaxed problem with respect to the fixed antenna positions problem we consider in this work. Furthermore, methods such as those of [13]-[16] do not make any provision for specifying a null depth. Thus, a direct comparison of the performance of these methods with our approach is not straightforward. Papers [9]-[12], on the other hand, allow one to set a null and perform the design accordingly. But these methods require the user to set the null depth, which means the optimisation criteria is fundamentally different from our approach. With our method, the null depth is calculated automatically by the adaptive algorithm as it attempts to make the signal and interference as orthogonal to each other as possible. Moreover, our algorithm can be used to reconfigure the array as the interference position changes relative to the desired signal which is a significant advantage of our strategy. Despite these major differences, a careful comparison of the performance between the proposed RAAA strategy and the reweighted l_1-norm method of [12] is possible. To this end, we set the peak and null positions at the DOAs of the target and interference respectively. The number of selected antennas for the reweighted l_1-norm is 41 and the selected subarray is shown in the lower plot of Fig. 9. The synthesized beampattern is also shown in Fig. 10 by the red dash curve. We can see that the mainlobe width is 4.4° and the PSL is -17dB, but the depth of the null is only -67.03dB. It is important to note that there is always a compromise between the mainlobe width and null depth. Therefore, given that the antennae positions are fixed, as we select them from a pre-determined array, the algorithm makes the null deeper by putting more emphasis on the null depth than the mainlobe width. Finally, we point out that the proposed RAAA strategy allows adaptivity and reconfigurability during operation, whereas the deterministic beampattern synthesis methods in [9]-[16] are fixed and usually calculated off-line at the array design stage.

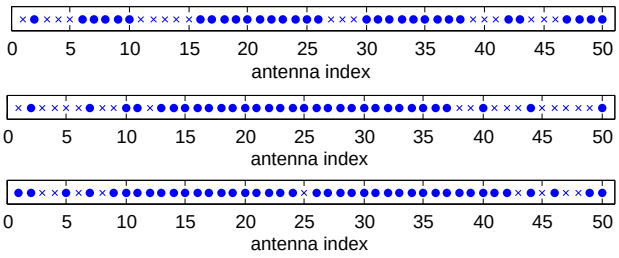

Fig. 9. Optimum Subarrays: with circle being selected and cross being discarded; the upper one is the CM 32-antenna subarray, the middle one is the 32-antenna subarray with quiescent pattern control, the lower one is the 41-antenna subarray with reweighted l_1-norm method.

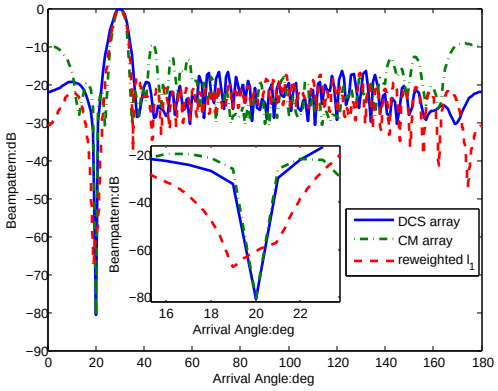

Fig. 10. Beampatterns: the blue solid curve is the MVDR beampattern of DCS subarray, the green dash-dot curve is the MVDR beampattern of CM subarray, the red dash curve is the synthesized beampattern of reweighted l_1-norm subarray. 1000 Monte Carlo runs were used in the simulation.

VI. Experimental Results

Next, we validate the theoretical and simulation results by using real experimental data. We use an 8-antenna circular array to collect the satellite signal data, as shown in Fig. 11. At the time of experiment, satellite SVN-25 was at azimuth and elevation angles of $\phi_s = 29^\circ, \theta_s = 35^\circ$ respectively. In the first scenario, we used Electromagnetic Interference (EMI) from a desktop computer as the interference source, which was coming from $\phi_j = 328^\circ, \theta_j = 0^\circ$. In order to create a case where the satellite signal is close to the interference, we use MATLAB to inject an interference into the collected clean data from $\phi_j = 35^\circ, \theta_j = 40^\circ$ as the second scenario. The interference-to-noise ratio are both more than $20dB$ in the two cases.

The effective C/N_0 was estimated by cross-correlating the received signal with the known GPS pseudo-random codes. Specifically, the Post-SINR is calculated by taking the cross correlation peak as the signal amplitude and the variance of the non-matching points in the cross-correlation function as the power of the noise. Additionally, the non-matching points are restricted to code offsets for which the sidelobes in the code cross-correlation function are more than 24 dB below

Fig. 11. The circular array used in the experiment and the EMI desktop interference.

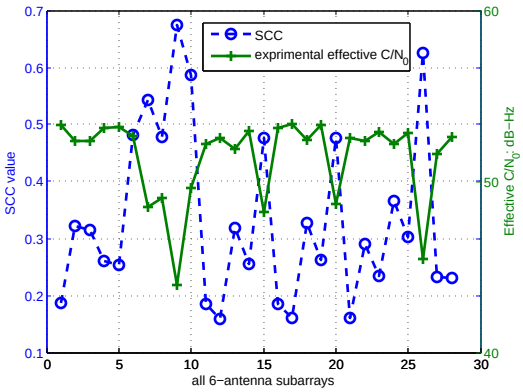

Fig. 12. SCC and corresponding experimental effective C/N_0 values of 28 different 6-antenna subarrays in the first scenario.

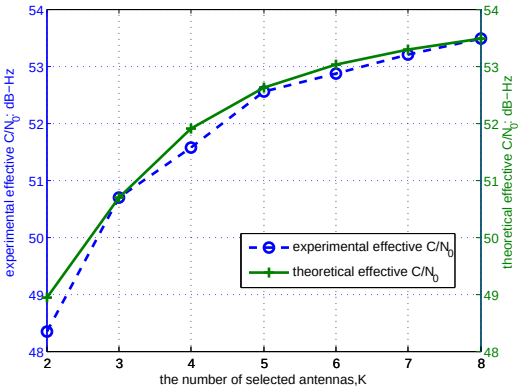

Fig. 13. Experimental and theoretical effective C/N_0 in scenario 1.

the matching point due to the auto-correlation sidelobes of the pseudo-random code [35]. The Post-SINR is then normalised to the noise power in a 1 Hz bandwidth to obtain the effective C/N_0.

The parameters used to calculate the theoretical effective C/N_0 in Eq. (10) are [36]:

1) the received satellite signal power is $P_s = -159$ dBW;
2) the IF bandwidth is 3 MHz;
3) the integration time T_d is 10 ms;
4) the noise power density is $N_0 = -203.9$ dB-Hz;
5) the sampling frequency is $f_s = 15.36$ MHz;

Firstly, the utility of array reconfiguration for performance improvement is validated by Fig. 12. Six antennas are chosen from the circular array in the second scenario and giving a total 28 candidate subarray configurations. The SCC and

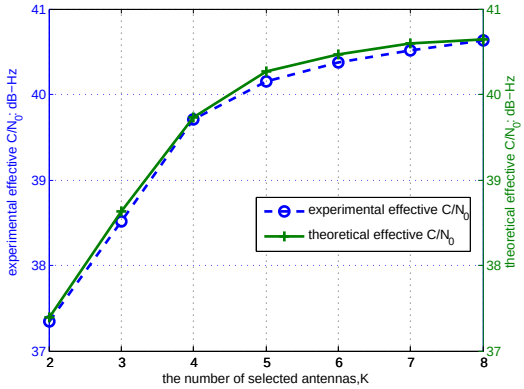

Fig. 14. Experimental and theoretical effective C/N_0 in scenario 2.

corresponding experimental effective C/N_0 values of all 28 subarrays are shown in Fig. 12. It is evident by comparing the two curves that when the SCC has a minimum value, the effective C/N_0 is maximum for the fixed number K. This confirms the inverse relationship between the SCC and effective C/N_0 derived in Eq. (10). Thus the subarray with the minimum SCC value is also the optimum subarray with the best performance. Also note from Fig. 12 that the optimum 6-antenna subarray gives 53.33 dB-Hz effective C/N_0, whereas the worst subarray yields an effective C/N_0 of 43.97 dB-Hz. This confirms the utility of array reconfiguration for improving the performance.

Next the antenna selection strategy is tested by Fig. 13 and Fig. 14. Only the data received from the selected K antennas are processed. In this way we can see the performance of subarrays with different numbers of selected antennas by changing the value K. The experimental results of the first and second scenarios are shown in Fig. 13 and Fig. 14 respectively. Firstly we can see that the experimental effective C/N_0 exhibits good agreement with the theoretical curve. Secondly, the effective C/N_0 shows a linear relationship with K in the first scenario, while it flattens out when K exceeds 5 in the second scenario. This coincides exactly with our simulation results in section V. Hence increasing the array size may not be necessary in some scenarios, an optimally configured subarray can preserve the performance with a significant cost reduction.

VII. Conclusion

In this paper, a reconfigurable adaptive antenna array strategy is proposed to utilise the array configuration as an additional DOF to improve array processing performance. The parameter, SCC, is introduced to characterise the effect of array configuration on the performance. The lower bound of the optimum SCC is derived with two relaxation methods and the non-linear relationship between the effective C/N_0 and the number of selected antennas is formulated. The trade-off curve between the performance and the cost gives information about the suitable value of K. Then, the proposed CM method was used to compose at least a $1/K^2$-suboptimum K-antenna subarray. The proposed DCS method can select an optimum subarray with a null towards the interference as well as achieve a controlled quiescent pattern. Both simulation and

experimental results demonstrate that the subarray can save both hardware and software cost with maximum performance preservation, given that K is suitably chosen and the subarray is optimally configured.

APPENDIX A
THE PROOF OF STRONG DUALITY

First we will show that Eq. (16) and Eq. (19) are a pair of duals, i.e. Eq. (19) is the bi-dual of the primal Eq. (13). We take the bi-dual variable $\mathbf{Y} \in R^{N+1}$,

$$\mathbf{Y} = \begin{bmatrix} \mathbf{X} & \mathbf{x} \\ \mathbf{x}^T & t \end{bmatrix} \succeq 0. \tag{31}$$

Then the Lagrangian associated with Eq. (16) is

$$\begin{aligned} & L(\zeta, \boldsymbol{\mu}, \upsilon, \mathbf{Y}) \\ = \; & \zeta + tr(\mathbf{Y} \bullet \begin{bmatrix} \frac{1}{K^2}\mathbf{W}_r + diag(\boldsymbol{\mu}) + \upsilon \mathbf{I} & -\frac{1}{2}\boldsymbol{\mu} \\ -\frac{1}{2}\boldsymbol{\mu}^T & -K\upsilon - \zeta \end{bmatrix}), \\ = \; & tr(\frac{1}{K^2}\mathbf{W}_r \mathbf{X}) + (1-t)\zeta + tr(diag(\boldsymbol{\mu})\mathbf{X}) - \boldsymbol{\mu}^T \mathbf{x} \\ + \; & \upsilon(tr(\mathbf{X}) - Kt). \end{aligned} \tag{32}$$

Its supremum with respect to $(\zeta, \boldsymbol{\mu}, \upsilon)$ is $+\infty$ unless $t = 1$, $tr(\mathbf{X}) - Kt = 0$ and the coefficient of each μ_i is zero. Thus the dual function is exactly Eq. (19). Let us denote by $val(\cdot)$ the optimum value of the optimization problem described in Eq. $(\cdot)$. Applying weak duality twice and the lifting procedure, we get

$$val(16) \leq val(19) \leq val(13). \tag{33}$$

It is worth mentioning that the first inequality often holds as an equality, as we show is the case here. Let us take the matrix

$$\mathbf{X} = \begin{bmatrix} K/N & K^2/N^2 & K^2/N^2 & \cdots & K^2/N^2 \\ K^2/N^2 & K/N & K^2/N^2 & \cdots & K^2/N^2 \\ \vdots & \vdots & \vdots & \vdots & \vdots \\ K^2/N^2 & K^2/N^2 & K^2/N^2 & \cdots & K/N \end{bmatrix}, \tag{34}$$

and $\mathbf{x} = [K/N, K/N, ..., K/N]^T$. Then

$$\begin{aligned} \mathbf{X} - \mathbf{x}\mathbf{x}^T &= \begin{bmatrix} \frac{K}{N} - \frac{K^2}{N^2} & 0 & \cdots & 0 \\ 0 & \frac{K}{N} - \frac{K^2}{N^2} & \cdots & 0 \\ 0 & 0 & \cdots & 0 \\ \vdots & \vdots & \vdots & \vdots \\ 0 & 0 & \cdots & \frac{K}{N} - \frac{K^2}{N^2} \end{bmatrix} \\ &\succ \mathbf{0}; \end{aligned} \tag{35}$$

Moreover, $tr(\mathbf{X}) = K$ and $tr(\mathbf{X}\mathbf{E}_i) - \mathbf{e}_i^T \mathbf{x} = 0, i = 1, 2, ..., N$ which satisfy Slater's condition in Eq. (19). Thus there is no duality gap between the two relaxation methods Eq. (16) and Eq. (19), and consequently $val(16) = val(19)$.

APPENDIX B
PROOF OF THEOREM 4.2

We prove Theorem 4.2 under two different cases which are divided according to the SCC value of the previous sub-problem. Let us assume the number of selected antennas $2 \leq K \leq N-2$, since the CM solution of choosing N and $N-1$ from N antennas is also the global optimum solution.

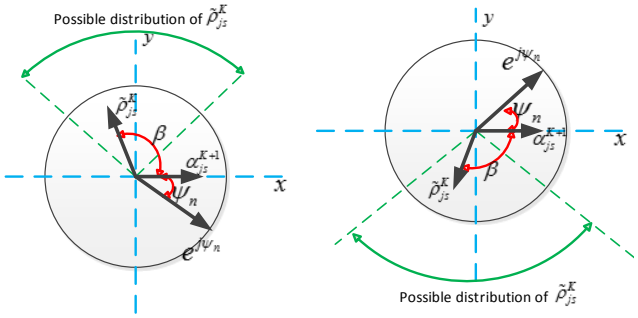

Fig. 15. Proof of Theorem 4.2: The optimum SCC of the $(N-K-1)_{th}$ sub-problem is α_{js}^{K+1}. The node $e^{j\Psi_n}$ is the closest antenna to α_{js}^{K+1}. $\tilde{\rho}_{js}^K$ is K times the optimum SCC value of the $(N-K)_{th}$ sub-problem. β is the angle between α_{js}^{K+1} and $\tilde{\rho}_{js}^K$. The range of $\tilde{\rho}_{js}^K$ that ensures its amplitude not exceed one is shown in the figure. Thus the amplitude of optimum SCC value for choosing K from N, i.e. $\alpha_{js}^K = \tilde{\rho}_{js}^K/K$, will not exceed $1/K$.

A. Case 1

Let us assume the SCC value returned by the $(N-K-1)_{th}$ subproblem of CM approach, i.e. selecting $K+1$ from N antennas, equal to zero, then the SCC value of the $(N-K)_{th}$ subproblem, i.e. selecting K from N antennas, is $1/K$. The reason is that when any antenna is removed from the $(K+1)$-antenna subarray, the sum of the remaining K exponentials is the exponential with opposite direction against the removed one due to the zero SCC. Thus the amplitude of the sum of K exponentials is one and the corresponding absolute SCC is $1/K$ after normalization.

B. Case 2

Let us suppose the optimum SCC of the $(N-K-1)_{th}$ sub-problem is

$$\alpha_{js}^{K+1} = \frac{1}{K+1}\sum_{i=1}^{N} \mathbf{x}(i) e^{j\psi_i} \neq 0, \tag{36}$$

where $\psi_i = \frac{2\pi}{\lambda}\mathbf{p}_i^T(\mathbf{u}_s - \mathbf{u}_j)$. Since the CM method deletes one antenna with the largest correlation to the remaining antennas, the correlation of the $l^{th}, 1 \leq l \leq N$ antenna with the remaining K antennas is given by

$$\begin{aligned} c^{K+1}(l) &= \frac{1}{K+1} real(\sum_{i=1}^{N} \mathbf{x}(i) e^{-j\psi_l} e^{j\psi_i}), \\ &= real(e^{-j\psi_l}\alpha_{js}^{K+1}), \end{aligned} \tag{37}$$

Let us assume without loss of generality that α_{js}^{K+1} is real, if not, then we rotate the axes to make it so. Then Eq. (37) can be rewritten as

$$c^{K+1}(l) = \alpha_{js}^{K+1}\cos(\psi_l), \tag{38}$$

Since α_{js}^{K+1} is common to all the $K+1$ antennas, the maximum correlation measurement corresponds to the minimum ψ_l, that is deleting the antenna with the smallest angle difference with respect to α_{js}^{K+1}, i.e. with respect to the x-axis here, denoted by $e^{j\psi_n}$ as shown in Fig. 15. Then we have that have $-\frac{\pi}{2} < \psi_n < \frac{\pi}{2}$, for if the absolute value of ψ_n was larger than $\frac{\pi}{2}$ then all of the exponentials would be in the other half

of the disk and the SCC cannot be along the positive real axis, thus violating our assumption.

It is clear that α_{js}^{K+1} is much less than the SCC value of selecting $K+1$ consecutive antennas, i.e.

$$\alpha_{js}^{K+1} \ll \frac{1}{K+1}\left|\frac{\sin[\pi d\Delta u(K+1)/\lambda]}{\sin(\pi d\Delta u/\lambda)}\right|, \tag{39}$$

Since we are analysing the performance of CM method under the case where it cannot converge globally, we assume the spatial separation $|\Delta u|$ is large such that,

$$0 < \alpha_{js}^{K+1} \leq \frac{2\cos\psi_n}{K+1}, \tag{40}$$

The SCC α_{js}^{K+1} can also be decomposed as the sum of $e^{j\psi_n}$ and $\tilde{\rho}_{js}^{K}$ as follows,

$$\alpha_{js}^{K+1} = \frac{1}{K+1}[\tilde{\rho}_{js}^{K} + e^{j\psi_n}], \tag{41}$$

where $\tilde{\rho}_{js}^{K}$ is the sum of K exponentials which are selected in the $(N-K)_{th}$ sub-problem. Because the projections of $e^{j\psi_n}$ and $\tilde{\rho}_{js}^{K}$ onto the y-direction need to cancel each other, we have that

$$\sin\psi_n + |\tilde{\rho}_{js}^{K}|\sin\beta = 0, \tag{42}$$

where β is the angle between α_{js}^{K+1} and $\tilde{\rho}_{js}^{K}$. Moreover, Eq. (41) can be rewritten as

$$\alpha_{js}^{K+1} = \frac{1}{K+1}(\cos\psi_n + |\tilde{\rho}_{js}^{K}|\cos\beta), \tag{43}$$

Combining Eq. (40), Eq. (42) and Eq. (43), we have that

$$-\cos\beta\frac{\sin\psi_n}{\sin\beta} \leq \cos\psi_n, \tag{44}$$

Next we consider to simply Eq. (44) from the following two cases,

$$-\psi_n \leq \beta \leq \pi + \psi_n \text{ if } -\frac{\pi}{2} < \psi_n \leq 0, \tag{45}$$

and

$$-\pi + \psi_n \leq \beta \leq -\psi_n \text{ if } 0 \leq \psi_n < \frac{\pi}{2}, \tag{46}$$

The possible distribution area of $\tilde{\rho}_{js}^{K}$ is shown in Fig.15. Thus the amplitude of $\tilde{\rho}_{js}^{K}$ is bounded within

$$|\sin\psi_n| \leq |\tilde{\rho}_{js}^{K}| \leq 1, \tag{47}$$

Therefore, the optimum SCC value of the $(N-K)_{th}$ sub-problem is bounded within

$$\frac{|\sin\psi_n|}{K} \leq |\alpha_{js}^{K}| = \frac{|\tilde{\rho}_{js}^{K}|}{K} \leq \frac{1}{K}. \tag{48}$$

Since the selection of K from N antennas needs totally $N-K$ sub-problems for CM approach and the effective C/N_0 is relevant to the squared SCC value, the upper bound of the distance between the objective value of CM solution and the global minimum is no more than $\frac{1}{K^2}$ in any scenario when $K \leq N-2$; is zero when $K = N$ or $K = N-1$.

REFERENCES

[1] H. Singh and R. Jha, "Trends in adaptive array processing," *International Journal of Antennas and Propagation*, vol. 2012, 2012.

[2] D. S. Jimmy LaMance, "Locata correlator-based beam forming antenna technology for precise indoor positioning and attitude," in *Proceedings of the 24th International Technical Meeting of The Satellite Division of the Institute of Navigation (ION GNSS 2011), September 2011*, pp. 2436–2445, 2011.

[3] W. Sun and M. Amin, "A self-coherence anti-jamming GPS receiver," *Signal Processing, IEEE Transactions on*, vol. 53, no. 10, pp. 3910–3915, 2005.

[4] M. Amin, L. Zhao, and A. Lindsey, "Subspace array processing for the suppression of FM jamming in GPS receivers," *Aerospace and Electronic Systems, IEEE Transactions on*, vol. 40, no. 1, pp. 80–92, 2004.

[5] M. Amin and W. Sun, "A novel interference suppression scheme for global navigation satellite systems using antenna array," *Selected Areas in Communications, IEEE Journal on*, vol. 23, no. 5, pp. 999–1012, 2005.

[6] A. Gershman and J. F. Bohme, "A note on most favorable array geometries for DOA estimation and array interpolation," *Signal Processing Letters, IEEE*, vol. 4, no. 8, pp. 232–235, 1997.

[7] Y. Hua and T. Sarkar, "A note on the Cramer-Rao bound for 2-D direction finding based on 2-D array," *Signal Processing, IEEE Transactions on*, vol. 39, no. 5, pp. 1215–1218, 1991.

[8] L. Cen, Z. Yu, W. Ser, and W. Cen, "Linear aperiodic array synthesis using an improved genetic algorithm," *Antennas and Propagation, IEEE Transactions on*, vol. 60, no. 2, pp. 895–902, 2012.

[9] S. Joshi and S. Boyd, "Sensor selection via convex optimization," *Signal Processing, IEEE Transactions on*, vol. 57, no. 2, pp. 451–462, 2009.

[10] H. Lebret and S. Boyd, "Antenna array pattern synthesis via convex optimization," *Signal Processing, IEEE Transactions on*, vol. 45, no. 3, pp. 526–532, 1997.

[11] S. Nai, W. Ser, Z. Yu, and H. Chen, "Beampattern synthesis for linear and planar arrays with antenna selection by convex optimization," *Antennas and Propagation, IEEE Transactions on*, vol. 58, no. 12, pp. 3923–3930, 2010.

[12] A. Massa and G. Oliveri, "Bayesian compressive sampling for pattern synthesis with maximally sparse non-uniform linear arrays," *Antennas and Propagation, IEEE Transactions on*, vol. 59, no. 2, pp. 467–481, 2011.

[13] Y. Liu, Z. Nie, and Q. Liu, "Reducing the number of elements in a linear antenna array by the matrix pencil method," *Antennas and Propagation, IEEE Transactions on*, vol. 56, no. 9, pp. 2955–2962, 2008.

[14] W. Du Plessis, "Weighted thinned linear array design with the iterative FFT technique," *Antennas and Propagation, IEEE Transactions on*, vol. 59, no. 9, pp. 3473–3477, 2011.

[15] W. Keizer, "Linear array thinning using iterative FFT techniques," *Antennas and Propagation, IEEE Transactions on*, vol. 56, no. 8, pp. 2757–2760, 2008.

[16] L. J. Griffiths and K. Buckley, "Quiescent pattern control in linearly constrained adaptive arrays," *Acoustics, Speech and Signal Processing, IEEE Transactions on*, vol. 35, no. 7, pp. 917–926, 1987.

[17] N. D. Sidiropoulos, T. N. Davidson, and Z.-Q. Luo, "Transmit beamforming for physical-layer multicasting," *Signal Processing, IEEE Transactions on*, vol. 54, no. 6, pp. 2239–2251, 2006.

[18] D. P. Palomar and Y. C. Eldar, *Convex optimization in signal processing and communications*. Cambridge university press New York, 2010.

[19] W.-K. Ma, T. N. Davidson, K. M. Wong, Z.-Q. Luo, and P.-C. Ching, "Quasi-maximum-likelihood multiuser detection using semi-definite relaxation with application to synchronous CDMA," *Signal Processing, IEEE Transactions on*, vol. 50, no. 4, pp. 912–922, 2002.

[20] L. A. Wolsey, "Integer programming," *IIE Transactions*, vol. 32, pp. 273–285, 2000.

[21] H. Marchand, A. Martin, R. Weismantel, and L. Wolsey, "Cutting planes in integer and mixed integer programming," *Discrete Applied Mathematics*, vol. 123, no. 1, pp. 397–446, 2002.

[22] T. H. Cormen, C. E. Leiserson, R. L. Rivest, and C. Stein, *Introduction to algorithms*. MIT press, 2001.

[23] J. Betz, "Effect of narrowband interference on GPS code tracking accuracy," in *Proceedings of the 2000 National Technical Meeting of The Institute of Navigation*, pp. 16–27, 2000.

[24] A. Balaei and E. Aboutanios, "Characterization of interference effects in multiple antenna GNSS receivers," in *Image and Signal Processing (CISP), 2010 3rd International Congress on*, vol. 8, pp. 3930–3934, IEEE, 2010.

[25] M. Li, A. Dempster, A. Balaei, C. Rizos, and F. Wang, "Switchable beam steering/null steering algorithm for CW interference mitigation in GPS C/A code receivers," *Aerospace and Electronic Systems, IEEE Transactions on*, vol. 47, no. 3, pp. 1564–1579, 2011.
[26] H. Lin, "Spatial correlations in adaptive arrays," *Antennas and Propagation, IEEE Transactions on*, vol. 30, no. 2, pp. 212–223, 1982.
[27] X. Wang and E. Aboutanios, "Reconfigurable adaptive linear array signal processing in GNSS applications," in *the 38th International Conference on Acoustics, Speech, and Signal Processing Proceedings (ICASSP)*, IEEE, 2013.
[28] R. Klemm, *Principles of space-time adaptive processing*. No. 159, Inspec/Iee, 2002.
[29] S. Boyd and L. Vandenberghe, *Convex Optimization*. Cambridge University Press, 2004.
[30] M. Grant and S. Boyd, *CVX Users' Guide*. 2012.
[31] A. d'Aspremont and S. Boyd, "Relaxations and randomized methods for nonconvex QCQPs," *EE392o Class Notes, Stanford University*, 2003.
[32] Y. Selén, H. Tullberg, and J. Kronander, "Sensor selection for cooperative spectrum sensing," in *New Frontiers in Dynamic Spectrum Access Networks, 2008. DySPAN 2008. 3rd IEEE Symposium on*, pp. 1–11, IEEE, 2008.
[33] H. Tuy, *Convex analysis and global optimization*, vol. 22. Springer, 1998.
[34] A. Beck, A. Ben-Tal, and L. Tetruashvili, "A sequential parametric convex approximation method with applications to nonconvex truss topology design problems," *Journal of Global Optimization*, vol. 47, no. 1, pp. 29–51, 2010.
[35] E. D. Kaplan and C. J. Hegarty, *Understanding GPS: principles and applications*. Artech House Publishers, 2006.
[36] X. Wang, E. Aboutanios, and M. Trinkle, "Subarray selection for adaptive array signal processing in GNSS applications," in *Proceedings of the 26th International Technical Meeting of The Satellite Division of the Institute of Navigation (ION GNSS+ 2013)*, pp. 2776–2785, ION, Nashville, TN, September 2013.

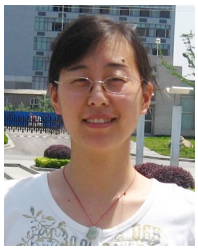

Xiangrong Wang received both the B.S. degree and the M.S. degree in electrical engineering from Nanjing University of Science and Technology, China, in 2009 and 2011, respectively. She is working toward the Ph.D. degree in electrical engineering in University of New South Wales, Sydney, Australia. She is currently a visiting research student in the Centre for Advanced Communications, Villanova University, USA. Her research interest include adaptive array processing, array beampattern synthesis, DOA estimation and convex optimization.

Elias Aboutanios (SM'11) received a Bachelor in Engineering in 1997, from UNSW and the PhD degree in 2003, from the University of Technology, Sydney (UTS). In 1993 he was awarded the UNSW Co-op Scholarship and the following year the Sydney Electricity scholarship. In 1998 he received an Australian Postgraduate Award and commenced his work toward the PhD degree at UTS. While at UTS he was a member of the CRC for Satellite Systems, working on the development of the Ka-Band Earth station. From 2003 to 2007, he was a research fellow with the Institute for Digital Communications at the University of Edinburgh where he conducted research on Space Time Adaptive Processing for radar target detection. He is currently a senior lecturer at UNSW. In 2011, Dr Aboutanios, received the Faculty of Engineering Teaching Excellence Award for developing the novel Design Proficiency subject that he teaches to final year undergraduates. Also in 2011, he led an international consortium in securing over $1M in funding to develop Australia's first masters in Satellite Systems Engineering. The project was completed in June 2013. Dr Aboutanios research interests include parameter estimation, algorithm optimization and analysis, adaptive and statistical signal processing and their application in the contexts of radar, GNSS, Nuclear Magnetic Resonance, and smart grids. He is the joint holder of a patent on frequency estimation.

Matthew Trinkle received the B.Eng (Hons) degree in Electrical Electronic Engineering and B.Sc. in Mathematical and Computer Science from the University of Adelaide, South Australia, in 1994 and 1995 respectively. From 1996 to 2004 he was with the Cooperative Research Centre for Sensor Signal and Information Processing mainly in the area of adaptive algorithms for GPS interference suppression. Since 2005 he has been with the University of Adelaide, mainly in the area of phased array processing for GPS, Radar and Acoustics.

Moeness G. Amin (F'01) received his Ph.D. degree in Electrical Engineering from University of Colorado in 1984. He has been on the Faculty of the Department of Electrical and Computer Engineering at Villanova University since 1985. In 2002, he became the Director of the Center for Advanced Communications, College of Engineering. He is a Fellow of the Institute of Electrical and Electronics Engineers (IEEE), 2001; Fellow of the International Society of Optical Engineering, 2007; and a Fellow of the Institute of Engineering and Technology (IET), 2010. Dr. Amin is a Recipient of the IEEE Third Millennium Medal, 2000; Recipient of the 2009 Individual Technical Achievement Award from the European Association of Signal Processing; Recipient of the 2010 NATO Scientific Achievement Award; Recipient of the Chief of Naval Research Challenge Award, 2010; Recipient of Villanova University Outstanding Faculty Research Award, 1997; and the Recipient of the IEEE Philadelphia Section Award, 1997. He was a Distinguished Lecturer of the IEEE Signal Processing Society, 2003-2004, and is currently the Chair of the Electrical Cluster of the Franklin Institute Committee on Science and the Arts. Dr. Amin has over 600 journal and conference publications in the areas of Wireless Communications, Time-Frequency Analysis, Sensor Array Processing, Waveform Design and Diversity, Interference Cancellation in Broadband Communication Platforms, satellite Navigations, Target Localization and Tracking, Direction Finding, Channel Diversity and Equalization, Ultrasound Imaging and Radar Signal Processing. He co-authored 18 book chapters. He is the Editor of the book "Through the Wall Radar Imagin" and "Compressive Sensing for Urban Radar," published by CRC Press in 2011 and 2014, respectively.

Dr. Amin currently serves on the Editorial Board of the IEEE Signal Processing Magazine. He also serves on the Editorial Board of the EURASIP Signal Processing Journal. He was a Plenary Speaker at ISSPIT-03, ICASSP-10, ACES-13, IET-13, EUSIPCO-13, STATOS-13, CAMSAP-13 and RADAR-14. Dr. Amin was the Special Session Co-Chair of the 2008 IEEE International Conference on Acoustics, Speech, and Signal Processing; the Technical Program Chair of the 2nd IEEE International Symposium on Signal Processing and Information Technology, 2002; was the General and Organization Chair of both the IEEE Workshop on Statistical Signal and Array Processing, 2000 and the IEEE International Symposium on Time-Frequency and Time-Scale Analysis, 1994. He was an Associate Editor of the IEEE Transactions on Signal Processing during 1996-1998; a member of the IEEE Signal Processing Society Technical Committee on Signal Processing for Communications during 1998-2002; a Member of the IEEE Signal Processing Society Technical Committee on Statistical Signal and Array Processing during 1995-1997. Dr. Amin was the Guest Editor of the Journal of Franklin Institute September-08 Special Issue on Advances in Indoor Radar Imaging; a Guest Editor of the IEEE Transactions on Geoscience and Remote Sensing May-09 Special Issue on Remote Sensing of Building Interior; a Guest Editor of the IET Signal Processing December-09 Special Issue on Time-Frequency Approach to Radar Detection, Imaging, and Classification; a Guest Editor of the IEEE Signal Processing Magazine November-13 and July-14 Special Issues on Time-frequency Analysis and Applications and Recent Advances in Synthetic Aperture Radar Imaging; and a Guest Editor of the EURASIP Journal on Advances in Signal Processing Special Issue on Sparse Sensing in Radar and Sonar Signal Processing.